sustainability

MDPI

Article

Inner Damping of Water in Conduit of Hydraulic Power Plant

Daniel Himr *,† **, Vladimír Habán** † **and David Štefan** †

Faculty of Mechanical Engineering, Brno University of Technology, Technická 2896/2, 616 69 Brno, Czech Republic; haban@fme.vutbr.cz (V.H.); stefan@fme.vutbr.cz (D.Š.)

* Correspondence: himr@fme.vutbr.cz

† These authors contributed equally to this work.

Abstract: The operation of any hydraulic power plant is accompanied by pressure pulsations that are caused by vortex rope under the runner, rotor–stator interaction and various transitions during changes in operating conditions or start-ups and shut-downs. Water in the conduit undergoes volumetric changes due to these pulsations. Compression and expansion of the water are among the mechanisms by which energy is dissipated in the system, and this corresponds to the second viscosity of water. The better our knowledge of energy dissipation, the greater the possibility of a safer and more economic operation of the hydraulic power plant. This paper focuses on the determination of the second viscosity of water in a conduit. The mathematical apparatus, which is described in the article, is applied to data obtained during commissioning tests in a water storage power plant. The second viscosity is determined using measurements of pressure pulsations in the conduit induced with a ball valve. The result shows a dependency of second viscosity on the frequency of pulsations.

Keywords: second viscosity; bulk viscosity; measurement; hydraulic power plant; conduit; pressure pulsations; dissipation; damping

Citation: Himr, D.; Habáne, V.; Štefan, D. Inner Damping of Water in Conduit of Hydraulic Power Plant. *Sustainability* **2021**, *13*, 7125. https://doi.org/10.3390/su13137125

Academic Editor: Tomonobu Senjyu

Received: 23 April 2021
Accepted: 14 June 2021
Published: 25 June 2021

1. Introduction

The unsteady flow in a pipeline is a phenomenon of great interest. It is not possible to avoid an unsteady flow when operating a hydraulic system. For example, a water turbine generates instability when it starts or stops, when the power changes, when a black-out occurs etc. All of these events induce transients connected to pressure pulsations. The magnitude of the pulsations depends on many factors, and it is necessary to examine these factors carefully in advance to prevent accidents and problems regarding operation or regulation.

Even the steady operation of a turbine generates pressure pulsations, which travel through the system. The pulsations are caused by vortex rope [1] or rotor–stator interactions when the runner blade is passing the guide vane [2]. These pulsations can induce severe vibrations of the structural parts in the system.

The behavior of hydraulic systems is usually simulated as one-dimensional flow described by continuity and momentum Equations (1) and (2), where the wave speed and viscosity are important parameters. The wave speed influences the magnitude of a pressure surge and the speed of a response of the system to any event. Viscosity defines energy dissipation via friction and is usually included in the friction loss coefficient.

$$\frac{\partial p}{\partial t} + \frac{a^2 \rho}{S} \frac{\partial Q}{\partial x} = 0, \tag{1}$$

$$\frac{\partial Q}{\partial t} + \frac{S}{\rho} \frac{\partial p}{\partial x} + \frac{\lambda}{2DS} |Q| Q = g_p S. \tag{2}$$

Experience and experiments of various researchers showed that energy loss defined only by the friction loss coefficient can be insufficient. Moreover, when water changes phase or dissolved air is released, energy is dissipated by the following mechanisms: unsteady

friction [3], friction in pipe material [4], fluid compression [5], when water changes phase or dissolved air is released [6,7]. Omitting these mechanisms can have a crucial impact on whether the analyzed system is deemed stable or unstable and on the selection of the method to control it.

The energy dissipation due to the compressibility of a liquid or gas can be expressed as a function of the bulk viscosity, which includes regular viscosity and the second coefficient of viscosity (second viscosity) (see Equation (3)).

$$b = \xi + \frac{2}{3}\eta. \tag{3}$$

Bulk viscosity is zero for dilute monoatomic gases according to Stokes' hypothesis. However, this assumption is not valid for other gases and liquids. An extensive review of bulk viscosity showed how the second viscosity influences equations describing fluid flow [5,8–12].

Thus far, many experiments have been performed to obtain the value of the bulk viscosity or the second viscosity. Karim [13] measured the second viscosity of water, methyl alcohol and ethyl alcohol in the 1950s. In recent work, Dukhin [14] compared three methods (Brillouin spectroscopy, laser transient grating spectroscopy and acoustic spectroscopy) for twelve liquids, including water. Holmes [15] investigated the dependence of the second viscosity of water on temperature using acoustic spectroscopy. He [16] performed similar experiments but used stimulated Brillouin scattering. All of the authors obtained similar results, but they did not describe any frequency dependence. However, all of the experiments were performed with very high pulsation frequencies (from 1 MHz to 1 GHz). The measurement of much lower pulsation frequencies (from 0.2 Hz to 10 kHz) is described in [17,18], where a hyperbolic dependence on frequency is described.

Determination of the second viscosity coefficient in a conduit of a hydraulic power plant is a main goal of the study. Measured data of the pressure pulsations are used. The mathematical background is briefly described in Section 2; a detailed description can be found in [17]. The measurement set-up is given in Section 3, and the following section discusses the obtained results.

2. Theory

A basic mathematical background is given in this section. One-dimensional flow is supposed in the pipe, which is a usual simplification in pipeline dynamics.

2.1. Continuity Equation

Generally, liquid flow can be described by the continuity equation and momentum equation. The continuity equation can be written in the following form:

$$\frac{\mathrm{d}\rho}{\mathrm{d}t}V + \rho\frac{\mathrm{d}V}{\mathrm{d}t} = 0. \tag{4}$$

Equation (5) provides a relationship between density and pressure.

$$\frac{\mathrm{d}p}{\mathrm{d}t} = a^2\frac{\mathrm{d}\rho}{\mathrm{d}t}. \tag{5}$$

For liquid in a pipe, Equation (4) can be adjusted into form (6) using Equation (5) when the Gauss–Ostrogradski formula is used.

$$\frac{1}{a^2}\frac{\mathrm{d}p}{\mathrm{d}t}S + \rho\frac{\partial Q}{\partial x} + \rho\frac{\int \vec{v}\vec{n}\mathrm{d}P}{\mathrm{dx}} = 0. \tag{6}$$

The integral in Equation (6) refers to the integration over the moving (deforming) pipe wall, where the inner surface is P, and the velocity is $\vec{v}$. The velocity can differ at different

points. The integral equals zero when the pipe is rigid. An ideal contact between the liquid and the pipe wall is assumed.

When a thin walled pipe is assumed, Equations (7) and (8) can be used to describe the stress and deformation of the wall.

$$\sigma = \frac{D}{2e}p, \tag{7}$$

$$v = \frac{D}{2}\frac{\partial \varepsilon}{\partial t}. \tag{8}$$

The model of the body in Figure 1 helps to define a relationship between the stress and deformation of the wall.

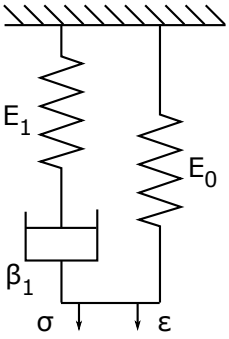

Figure 1. Model of the pipe wall.

The final shape of the continuity Equation (9) can be found after a Laplace transformation of Equations (6)–(8), where the complex wave speed is a function of the complex Young's modulus (see Equations (10) and (11)). A circular cross-section of the pipe is assumed.

$$0 = \frac{\rho a_c^2}{S}\frac{\partial \bar{Q}}{\partial x} + s\bar{p}, \tag{9}$$

$$a_c = a\sqrt{\frac{E_c e}{E_c e + a^2 \rho D}}, \tag{10}$$

$$E_c = E_0 + \frac{sE_1\beta_1}{E_1 + s\beta_1}. \tag{11}$$

2.2. Momentum Equation

The momentum Equation for liquid (12) includes energy loss in the tensor Π.

$$\rho\frac{\partial \vec{v}}{\partial t} + \rho\vec{v}\,\mathrm{grad}\vec{v} - \mathrm{div}\Pi + \mathrm{grad}p = 0. \tag{12}$$

Tensor Π describes the energy loss due to friction and compression (see Equation (13)).

$$\mathrm{div}\Pi = \eta\Delta\vec{v} + (\eta + \xi)\mathrm{grad}\ \mathrm{div}\vec{v}. \tag{13}$$

It is possible to neglect the second term in Equation (12) when the liquid velocity is much lower than the wave speed. Then, one-dimensional flow in a pipe with a circular cross-section can be described by Equation (14).

$$\frac{\partial Q}{\partial t} - \frac{2\eta + \xi}{\rho}\frac{\partial^2 Q}{\partial x^2} - \left(\frac{4\eta}{\rho D^2}\right)^2 \int_0^t \Gamma(t-\tau)Q\mathrm{d}\tau + \frac{S}{\rho}\frac{\partial p}{\partial x} = 0. \tag{14}$$

Memory function Γ expresses the energy loss due to an unsteady velocity profile. It has a great impact on liquids with high viscosity (oil) or on flow in a capillary. Usually,

it can be neglected, because its effect is much smaller than that of the second viscosity influence [19,20]. Thus, the final shape of the momentum equation can be written after a Laplace transformation when the flow rate derivation is substituted using Equation (9).

$$\frac{S}{\rho}\left[1+(2\eta+\xi)\frac{s}{a_c^2}\right]\frac{\partial \bar{p}}{\partial x}+s\bar{Q}=0. \tag{15}$$

2.3. Second Viscosity

The solution of Equations (9) and (15) can be written using a transfer matrix $\mathbf{T}(x,s)$ with a 2×2 size as follows:

$$\begin{pmatrix} \bar{Q} \\ \bar{p} \end{pmatrix} = \mathbf{T}(x,s)\begin{pmatrix} \bar{Q} \\ \bar{p} \end{pmatrix}_{x=0}. \tag{16}$$

Therefore, when the boundary conditions for $x = 0$ are known (beginning of the pipe), it is possible to obtain the Laplace transformations of the pressure and flow rate wherever in the pipe. The transfer matrix contains all of the properties and geometrical parameters of the pipe line and flowing fluid, including the wave speed and second viscosity.

When the boundary conditions and conditions in another place are known (for example, from an experiment), it is possible to use an appropriate optimization method to find some elements of the transfer matrix. This is a good way to compute second viscosity and wave speed.

These parameters can also be obtained using eigenvalues of the transfer matrix. The first step is to obtain a response of the system to an impulse. This is the experimental part. The impulse can be induced with the valve (when water flows, the valve closing causes pressure pulsations). The eigenvalue of the system can be determined from a Fourier transformation of the measured pressure pulsations, and this is a complex number. The imaginary part is the same as the eigen angular frequency of the pulsations. The real part can be computed from the corresponding amplitude of a system of a single degree of freedom (see Equation (17) and Figure 2).

$$s = \frac{\pi}{\sqrt{3}}\Delta f \pm i2\pi f. \tag{17}$$

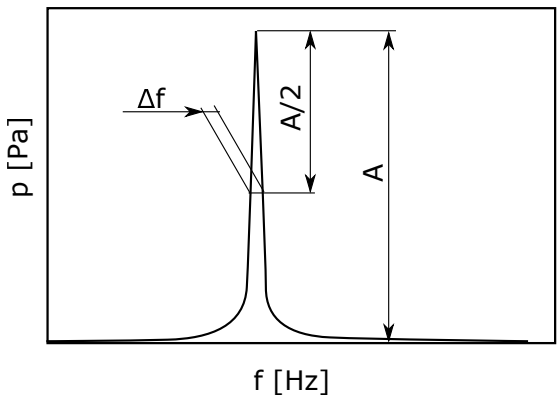

Figure 2. Determination of the real part of the eigenvalue.

The eigenvalue of the system equals the eigenvalue of the transfer matrix. The wave speed and second viscosity can be changed to meet this requirement. The transfer matrix can be written in various forms that include properties of the system (plain fluid, fluid + pipe, fluid + pipe with added mass). Detailed mathematical analysis is described in [17], and the chosen form of the transfer matrix with fluid properties has a form (18).

$$\mathbf{T}(x,s) = \begin{pmatrix} \cosh\left(\sqrt{\frac{s\cdot B}{A\cdot C}}\cdot x\right) & -\sqrt{\frac{s\cdot A}{B\cdot C}}\cdot\sinh\left(\sqrt{\frac{s\cdot B}{A\cdot C}}\cdot x\right) \\ -\sqrt{\frac{B\cdot C}{s\cdot A}}\cdot\sinh\left(\sqrt{\frac{s\cdot B}{A\cdot C}}\cdot x\right) & \cosh\left(\sqrt{\frac{s\cdot B}{A\cdot C}}\cdot x\right) \end{pmatrix}, \tag{18}$$

where coefficients A, B, C stand for:

$$A = \frac{S}{\rho} + \frac{2\cdot\eta+\zeta}{\rho^2}\cdot\frac{S\cdot s}{a^2}, \tag{19}$$

$$B = s - \frac{s\cdot \mathrm{J}_1\left(\frac{D}{2}\cdot \mathrm{i}\cdot\sqrt{\frac{s\cdot\rho}{\eta}}\right)}{s\cdot \mathrm{J}_1\left(\frac{D}{2}\cdot \mathrm{i}\cdot\sqrt{\frac{s\cdot\rho}{\eta}}\right) - \frac{D}{4}\cdot \mathrm{i}\cdot\sqrt{\frac{s\cdot\rho}{\eta}}\cdot \mathrm{J}_0\left(\frac{D}{2}\cdot \mathrm{i}\cdot\sqrt{\frac{s\cdot\rho}{\eta}}\right)}, \tag{20}$$

$$C = \frac{a^2\cdot\rho}{S}. \tag{21}$$

Second viscosity and wave speed have to be optimized to obtain the zero determinant of the transfer matrix.

3. Measurement

The storage hydraulic power plant Dlouhé Stráně is the most powerful hydraulic power plant in the Czech Republic. It has two Francis turbines (2 × 325 MW), which can also work as pumps. The turbines collect water from a bottom reservoir built on Dlouhá Desná river and pump it into a top reservoir on the top of Dlouhé Stráně mountain. The geodetic head is 510–534 m, and the flow rate during the turbine operation is 2 × 68.5 m^3/s. Each turbine has its own conduit with a length of 1547 and 1495 m and a diameter of 3.6 m. A simplified scheme is shown in Figure 3.

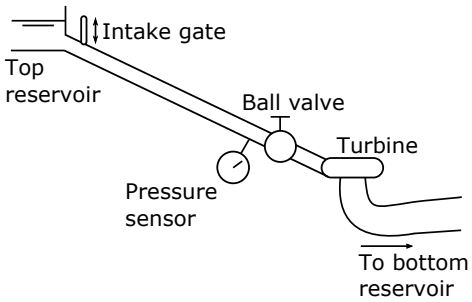

Figure 3. Scheme of one conduit with the turbine.

Measurement of the pressure pulsations was performed in November 2011 as a part of the commissioning tests in relation to turbine modernization. The obtained data primarily were used to determine the initial flow rate using the time-pressure method (Gibson's method). Twenty-eight sets of data were gathered, including the regular stop, emergency stop and disconnection of the electric network. Only data from the regular stop of the turbine are usable for second viscosity computations (see Figure 4).

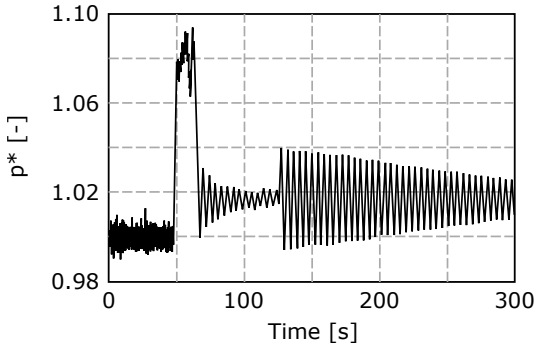

Figure 4. Pressure upstream of the ball valve during the regular stop.

Steady operation continued until the 50th second. Then, guide vanes started to close and caused a pressure surge that was 9% above the initial value. The guide vanes completely closed within 20 s. The ball valve upstream of the turbine also started to close but more slowly than the guide vanes. The pressure pulsations were damped until the 125th second. The ball valve finally closed at this time. The following pulsations correspond to an unsteady flow in a simple pipe with the boundary condition of constant pressure at the upstream end and a zero flow rate at the downstream end. These pulsations are mathematically well described and are usable for the evaluation of the wave speed and second viscosity (see Figure 5).

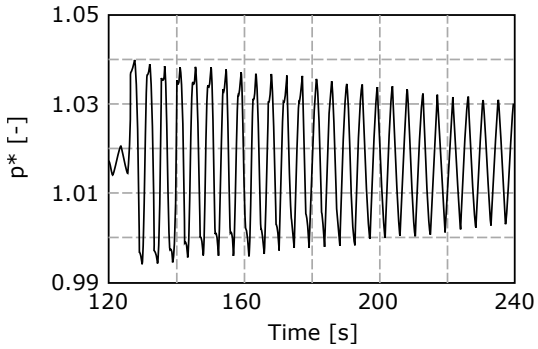

Figure 5. Pressure upstream of the ball valve during the regular stop after the ball valve fully closed.

The emergency stop is the same as the regular stop, but when the guide vanes finish closing, the intake gate also closes. The obtained pressure data are not appropriate for second viscosity evaluation, because the pulsations are strongly damped. Tests of closing after electricity disconnection also did not provide any usable data. Again, the system closed the intake gate, and the pulsations were damped too quickly.

4. Evaluation

Pressure oscillations after the 125th second were subject to discrete Fourier transformation, and then the eigen frequencies were determined. Table 1 shows the first seven eigen frequencies obtained from the measured pressure using Equation (17).

Table 1. Eigenvalues and corresponding shapes of pressure pulsations.

Real Part (α), Imaginary Part (ω), Frequency (f)	Shape of Pressure Amplitudes along the Conduit
α = 0.0121522 rad/s ω = 1.403 rad/s f = 0.223 Hz	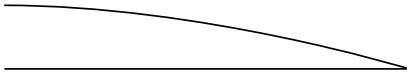
α = 0.01469911 rad/s ω = 4.235 rad/s f = 0.674 Hz	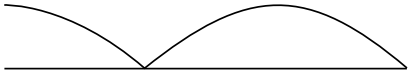
α = 0.03323047 rad/s ω = 6.991 rad/s f = 1.113 Hz	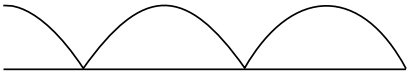
α = 0.03837075 rad/s ω = 9.792 rad/s f = 1.558 Hz	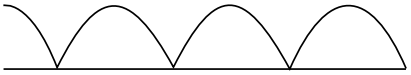
α = 0.04869796 rad/s ω = 12.610 rad/s f = 2.007 Hz	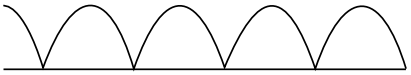
α = 0.08408768 rad/s ω = 15.355 rad/s f = 2.444 Hz	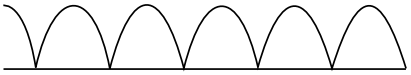
α = 0.07548372 rad/s ω = 18.156 rad/s f = 2.890 Hz	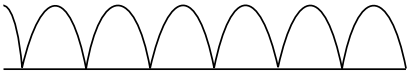

The shapes of the pressure amplitude along the conduit are shown in the right column. The left end is the location of the valve; thus, the pressure always has maximal amplitude there. The right end corresponds to the reservoir that maintains constant pressure there.

When the eigenvalues of the system are known, it is possible to determine the wave speed and second viscosity, which satisfy Equation (16). The values were obtained from eigenvalues in Table 1, and they are plotted in Figures 6 and 7.

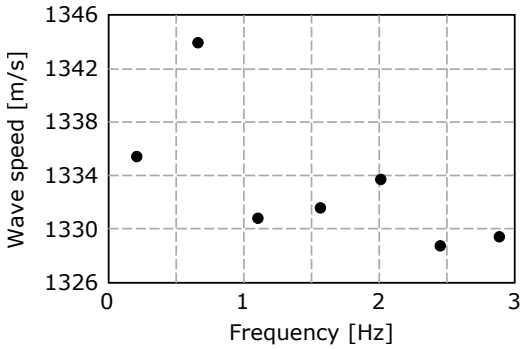

Figure 6. Wave speed with different frequencies.

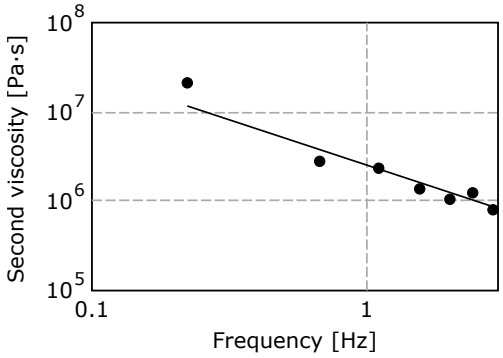

Figure 7. Second viscosity for different frequencies.

It is clear that the wave speed is independent of the frequency. The scattering is 1.1% from the mean value. The uncertainty was 0.2% of the sensor range, its time constant was 0.005 s and it was directly mounted on the pipe wall. Unlike the wave speed, the second viscosity strongly depends on the frequency. One can easily find a hyperbolic function that satisfactorily corresponds to the obtained values. Figure 7 is on a logarithmic scale; therefore, the hyperbola appears as a line (see following equation). The obtained result corresponds to [17].

$$\xi = \frac{C}{f}. \tag{22}$$

Bubbles of free air in the water have an impact on the wave speed and second viscosity [21]; however, in this case, the water had been pumped up and down several times before this measurement. Therefore, there was a very low level of air content, and it is possible to neglect its influence.

5. Summary

This paper describes an evaluation of the second viscosity of water. Pressure pulsations in a conduit of a storage power plant were measured at the ball valve. The measurement was performed as a part of commissioning tests and served for computations of the flow rate using the time-pressure method; however, it was also possible to use it for the evaluation of the second viscosity. The second viscosity was found from the eigenvalue of the conduit. The result showed a hyperbolic dependence of second viscosity on the frequency.

The presented methodology could be transferred to other hydraulic machines of any scale in order to verify the hydraulic system in which the machine will operate. This is necessary for economic and safer operations.

Author Contributions: Conceptualization, V.H.; methodology, V.H.; validation, D.H. and D.Š.; formal analysis, D.Š.; investigation, V.H. and D.H.; resources, D.Š.; data curation, V.H. and D.H.; writing—original draft preparation, D.H. and D.Š.; funding acquisition, D.H. and D.Š. All authors have read and agreed to the published version of the manuscript.

Funding: This paper was supported by the projects "Computer Simulations for Effective Low-Emission Energy" funded as project no. CZ.02.1.01/0.0/0.0/16_026/0008392 by Operational Programme Research, Development and Education, Priority axis 1: Strengthening capacity for high-quality research and project no. FSI-S-20-6235 "The Fluid Mechanics Principle Application as a Sustainable Development Tool."

Institutional Review Board Statement: Not applicable.

Informed Consent Statement: Not applicable.

Data Availability Statement: Restrictions apply to the availability of these data. Data were obtained from OSC, a.s. and are available from the authors only with the permission of OSC, a.s.

Conflicts of Interest: The authors declare no conflicts of interest.

Symbols

The following symbols are used in this manuscript:

a	wave speed
b	bulk viscosity
D	pipe diameter
E	Young's modulus
e	pipe wall thickness
f	frequency
g_p	gravity acceleration projection to pipe axis
i	imaginary unit

J_0	Bessel function
J_1	Bessel function
n	normal vector oriented out of liquid
P	pipe wall area
p	pressure
Q	flow rate
S	pipe cross-section
s	parameter of Laplace transformation
T	transfer matrix
t	time
V	volume
v	velocity
x	longitudinal coordinate
β	pipe wall damping
ε	deformation
η	dynamic viscosity
λ	friction coefficient
ξ	second viscosity
ρ	density
σ	stress
ω	angular velocity

Subscripts:

c	complex number
0	see Figure 1
1	see Figure 1

Superscripts:

*	value divided by steady value
-	variable after Laplace transformation

References

1. Alligne, S.; Nicolet, C.; Tsujimoto, Y.; Avellan, F. Cavitation surge modelling in Francis turbine draft tube. *J. Hydraul. Res.* **2014**, *52*, 399–411. [CrossRef]
2. Liu, H.; Ouyang, H.; Wu, Y.; Tian, J.; Du, Z. Investigation of unsteady flows and noise in rotor-stator interaction with adjustable lean vane. *Eng. Appl. Comp. Fluid* **2014**, *8*, 299–307. [CrossRef]
3. Vítkovský, J. P.; Bergant, A.; Simpson, A.R.; Lambert, M.F. Systematic evaluation of one-dimensional unsteady friction models in simple pipelines. *J. Hydraul. Eng.* **2006**, *132*, 696–708. [CrossRef]
4. Keramat, A.; Kolahi, A.G.; Ahmadi, A. Waterhammer modelling of vicoelastic pipes with a time-dependent Poissons's ratio. *J. Fluid. Struct.* **2013**, *43*, 164–178. [CrossRef]
5. Pochylý, F.; Habán, V.; Fialová, S. Bulk viscosity—Constitutive equations. *Int. Rev. Mech. Eng.* **2011**, *5*, 1043–1051.
6. Cannizzaro, D.; Pezzinga, G. Energy dissipation in transient gaseous cavitation. *J. Hydraul. Eng.* **2005**, *131*, 724–732. [CrossRef]
7. Jablonská, J. Compressibility of the fluid. *EPJ Web. Conf.* **2014**, *67*, 322–327. [CrossRef]
8. Graves, R.E.; Argrow, B.M. Bulk viscosity: Past to present. *J. Thermophys. Heat Tr.* **1999**, *13*, 337–342. [CrossRef]
9. Dellar, P.J. Bulk and shear viscosities in lattice Boltzmann equations. *Phys. Rev. E* **2001**, *64*, 11. [CrossRef] [PubMed]
10. Zuckerwar, A.J.; Ash, R.L. Volume viscosity in fluids with multiple dissipative processes. *Phys. Fluids* **2009**, *21*, 12. [CrossRef]
11. Marner, F.; Scholle, M.; Herrmann, D.; Gaskell, P.H. Competing Lagrangians for incompressible and compressible viscous flow. *Roy Soc. Open Sci.* **2019**, *6*, 14. [CrossRef] [PubMed]
12. Scholle, M. A discontinuous variational principle implying a non-equilibrium dispersion relation for damped acoustic waves. *Wave Motion* **2020**, *98*, 11. [CrossRef]
13. Karim, S.M. Second viscosity coefficient of liquid. *J. Acoust. Soc. Am.* **1953**, *25*, 997–1002. [CrossRef]
14. Dukhin, A.S.; Goetz, P.J. Bulk viscosity and compressibility measurement using acoustic spectroscopy. *J. Chem. Phys.* **2009**, *130*, 13. [CrossRef] [PubMed]
15. Holmes, M.J.; Parker, N.G.; Povey, M.J.W. Temperature dependence of bulk viscosity in water using acoustic spectroscopy. *J. Phys. Conf. Ser.* **2011**, *269*, 7. [CrossRef]
16. He, X.; Wei, H.; Shi, J.; Liu, J.; Li, S.; Chen, W.; Mo, X. Experimental measurement of bulk viscosity of water based on stimulated Brillouin scattering. *Opt. Commun.* **2012**, *285*, 4120–4124. [CrossRef]

17. Himr, D.; Habán, V.; Fialová, S. Influence of second viscosity on pressure pulsation. *Appl. Sci.* **2019**, *9*, 5444. [CrossRef]
18. Dörfler, P. Pressure wave propagation and damping in a long penstock. In Proceedings of the 4th International Meeting on Cavitation and Dynamic Problems in Hydraulic Machinery and Systems, Belgrade, Serbia, 26–28 October 2011.
19. Zielke, W. Frequency-dependent friction in transient pipe flow. *J. Basic Eng.* **1968**, *90*, 109–115. [CrossRef]
20. Zielke, W. Frequency Dependent Friction in Transient Pipe Flow. Ph.D. Thesis, The University of Michigan, Ann Arbor, MI, USA, 1966.
21. Záruba, J. *Water Hammer in Pipe-Line Systems*, 2nd ed.; Academia: Prague, Czech Republic, 1993.